Int. J. Electrochem. Sci., 12 **(2017)** 8609 – 8621, doi: 10.20964/2017.09.03

International Journal of
ELECTROCHEMICAL
SCIENCE
www.electrochemsci.org

$LiNi_{0.5}Mn_{1.45}Zn_{0.05}O_4$ with Excellent Electrochemical Performance for Lithium Ion Batteries

Hongyan Sun[1,2], *Xin Kong*[1,2], *Baosen Wang*[1,2], *Tingbi Luo*[1,2], *Guiyang Liu*[1,2,*]

[1] Department of Chemistry, College of Science, Honghe University, Mengzi, 661199, Yunnan, China
[2] Local Characteristic Resource Utilization and New Materials Key Laboratory of Universities in Yunnan, Honghe University, Mengzi 661199, Yunnan, China.
[*]E-mail: liuguiyang@tsinghua.org.cn

Received: 24 May 2017 / *Accepted:* 26 June 2017 / *Published:* 13 August 2017

Pure $LiNi_{0.5}Mn_{1.45}Zn_{0.05}O_4$ with a mixture of ordered and disordered phase has been successfully synthesized by a low temperature solution combustion synthesis method at 700℃. The phase structure and micro morphologies are investigated by X-ray powder diffraction(XRD), infrared spectroscopy(FT-IR) and scanning electron microscopy(SEM). The electrochemical properties are studied by cyclic voltammetry(CV), electrochemical impedance spectroscopy(EIS) and galvanostatic charge-discharge testing. The results indicate that the substitution of Zn on Mn site in the $LiNi_{0.5}Mn_{1.5}O_4$ can improve the cycling stability both at room temperature and even at elevated temperature 55℃ and the rate capability significantly. The initial specific capacity at 1C rate of $LiNi_{0.5}Mn_{1.45}Zn_{0.05}O_4$ is 140.4mAh/g, and can remain 95% after 400 cycles at room temperature and 92.9% after 100 cycles at 55℃. The specific capacity of $LiNi_{0.5}Mn_{1.45}Zn_{0.05}O_4$ is high to 125.3mAh/g at 10C, and the capacity retention is still 95.4% after 100 cycles at 10C compared with the first cycle at 10C. The excellent performance of $LiNi_{0.5}Mn_{1.45}Zn_{0.05}O_4$ is ascribed to its better crystallinity, higher conductivity and higher lithium diffusion coefficient(D_{Li}).

Keywords: Lithium-ion batteries, $LiNi_{0.5}Mn_{1.5}O_4$ spinels, Zn doping, rate capability

1. INTRODUCTION

High capacity, high rate capability and long life contribute to the success commercial applications for electric vehicles (EVs) and hybrid electric vehicles(HEVs) of lithium-ion batteries. In particular, $LiNi_{0.5}Mn_{1.5}O_4$(LNMO) spinels are being considered for positive electrode because of their high voltage, safety and cycling stability [1-4]. Unfortunately, the rate capability of LNMO with ordered $P4_332$ crystal structure and the cycling stability of LNMO at elevated temperatures are not

satisfactory and need to be significantly improved [5-7]. To solve these problems, various strategies have been attempted by researchers such as synthesis method, surface coating and doping, and so on.

The electrochemical performance of LNMO is greatly affected by synthesis methods and preparation conditions[5]**.** The synthesis methods mainly include solid-state reaction and solution synthetic methods. The phase structure, micro-morphology and performance of LNMO are very different via different synthesis methods. Zhu et al.[8]prepared LNMO by oxalic pretreated solid-state process. The materials delivered an initial discharge capacity of 136.9 $mAhg^{-1}$ and capacity retention of 93.4% after 300 cycles at 0.3C. Liu et al.[9] synthesized single phase LNMO with solution combustion synthesis method. The product exhibited excellent rate properties and large lithium diffusion coefficient. The capacity is 130 and 113 $mAhg^{-1}$ at 1C and 10C, respectively. After 100 cycles, the retentions were 97.5% and 99.7%, respectively. Surface coating has also been considered as one effective and controllable approach to stabilize the electrode/electrolyte interface and reduce the side reactions[10]. The different coating materials mainly including carbon materials, oxides, metals, lithium compounds and so on can retard the side reactions between the electrode and electrolyte and to further diminish the electrode dissolution during cycling test to some extent.

Doping has been proved to be one of the most efficient routes to improve the electrochemical performance of LNMO. To the best of our knowledge, the doping elements mainly include Na^{+}[11], Mg^{2+}[12], Cu^{2+}[13], Zn^{2+}[14], Al^{3+}[12], Cr^{3+}[15], Fe^{3+}[16], etc.. The LNMO spinels doped by Mg or Al all have improved electrochemical performance as we reported previously. Meanwhile, $LiNi_{0.5}Mn_{1.4}Mg_{0.1}O_4$ shows better rate capability and cycling stability than $LiNi_{0.5}Mn_{1.5}O_4$. Zhong et al.[6] synthesized the Al-substituted $LiNi_{0.5-x}Mn_{1.5-x}Al_{2x}O_4$, $LiNi_{0.5-x}Mn_{1.5}Al_xO_4$ and $LiNi_{0.5}Mn_{1.5-x}Al_xO_4$. They found that the cyclic performance and rate capability have been improved substantially compared with the Al-free LNMO sample. Wang et al.[11] reported a Na-doped $Li_{1-x}Na_xNi_{0.5}Mn_{1.5}O_4$ with a mixture of disordered Fd-3m phase and ordered $P4_332$ phase. The products show higher rate capabilities and cycling stability than those of the pristine LNMO electrode at elevated temperature.

The substitution of Zn for Ni site in LNMO spinel was firstly put forward by Manthiram et al.[14]. The $LiZn_{0.08}Ni_{0.42}Mn_{1.5}O_4$ sample had better cyclability than that of the Zn-free LNMO. Based on this, Yang et al.[17] systematically investigated the effect of different Zn doping amount for Ni site on the structure and electrochemical performance of LNMO. The result showed that the $LiZn_{0.08}Ni_{0.42}Mn_{1.5}O_4$ with pure disordered space group phase delivered improved cycle-life and rate capability at normal and elevated temperatures compared with Zn-free LNMO. However, the $LiZn_xNi_{0.5-x}Mn_{1.5}O_4$ samples showed decreasing specific capacities with increasing x because of the substitution of Zn^{2+} for Ni^{2+} lowering the Ni content and then giving rise to the decreased capacity at the ~4.7V plateau. Moreover, the cycle stability especially at high temperature of $LiZn_xNi_{0.5-x}Mn_{1.5}O_4$ needs to be further improved. The capacity retention of the best sample $LiZn_{0.08}Ni_{0.42}Mn_{1.5}O_4$ that they reported was only 60% over 100 cycles at 60 ^oC.

Noticing that Zn doping could indeed improve the electrochemical performance of LNMO, and little previous works have involved the substitution of Zn^{2+} for Mn^{4+} in LNMO. In this paper, the Zn^{2+} substitution for Mn^{4+} was investigated. On one hand, the substitution of Zn on Mn site may aviod the decreasement of the Ni content, which results in low capacity. On the other hand, it can lower the possibility of the formation of Mn^{3+} ions from Mn^{4+} during discharging process or oxygen loss.

According to the failure mechanism of LNMO reported by J.H. Kim[18], the Mn^{3+} existing in LNMO would make it suffer more severe Mn dissolution problem during cycle which can bring the obvious capacity dagradation, especially at high temperature. So we deduce that the substitution of Zn^{2+} on Mn^{4+} in $LiNi_{0.5}Mn_{1.5}O_4$ will display high specific capacity, excellent rate capability and cycling performance.

2. EXPERIMENTAL

2.1 Preparation

The $LiNi_{0.5}Mn_{1.45}Zn_{0.05}O_4$ (or $LiNi_{0.5}Mn_{1.5}O_4$ for compariation) powders were prepared by a modified solution combustion synthesis method as previously described[10, 12]. Raw materials of $LiNO_3$, CH_3COOLi, $Ni(NO_3)_2$, $(CH_3COO)_2Ni$, $Mn(NO_3)_2$, $(CH_3COO)_2Mn$ and $(CH_3COO)_2Zn$ with a stoichimetric molar ratio of 0.5:0.5:0.25:0.25:0.725:0.725:0.05 (or 0.5:0.5:0.25:0.25:0.75:0.75:0) were dissolved in distilled water to obtain a green solution. Then the solution was combusted in a muffle furnace at 700℃ and then kept at 700℃ for 14h. After cooling down to room temperature in the furnace naturally, the final spinel materials were obtained. All the treatment processes were carried out in air atmosphere.

2.2 Material characterization

Powder X-ray diffraction (XRD, PANalytical X'pert pro, Cu-Kα radiation) and Fourier transformed infrared spectroscopy(FTIR, PerkinElmer, with KBr pellets) were employed to characterize the structure of $LiNi_{0.5}Mn_{1.45}Zn_{0.05}O_4$ and $LiNi_{0.5}Mn_{1.5}O_4$ samples. The field emission scanning electron microscopy(SEM, FEI Quanta FEG 250) was used to observe the morphologies of products.

2.3 Electrochemical measurements

Electrochemical performance was evaluated with CR2025-type coin cells. The working electrodes were prepared by casting a slurry of 75wt.% active materials, 15wt.% conductive carbon and 10wt.% polyvinylidene difluoride(PVDF) binder dissolved in N-methyl-2-pyrrolidinone(NMP) on aluminum foil and dried at 120℃ under vacuum for 12h. A Li foil used as both the counter and reference electrode. CR2025-type coin cells were assembled by sandwiching a porous Celgard polyethylene separator between the working electrode and Li metal foil in a high purity Ar-filled glove box. The electrolyte was 1M $LiPF_6$ in a mixed solution of ethylene carbonate(EC) and dimethyl carbonate(DEC) with a weight ratio of 1:1.

Cells were galvanostatically charged and discharged on a battery test system(LANHE CT2001A instrument, Wuhan, China) at room temperature and 55℃ in the voltage range of 3.5-5.0V at different C rates(1C=150mA/g). Cyclic voltammogram(CV) of the cells was measured using an

electrochemical workstation(CHI 660) in a voltage range of 3.5-5.0V at a scan rate from 0.1 to 0.5mV/s. Electrochemical impedance spectroscopy (EIS) of the products was carried out by an electrochemical workstation(CHI 660) with an amplitude of ac voltage 5mV and a frequency range from 100 kHz to 0.1 Hz.

3. RESULTS AND DISCUSSION

3.1 Phase composition

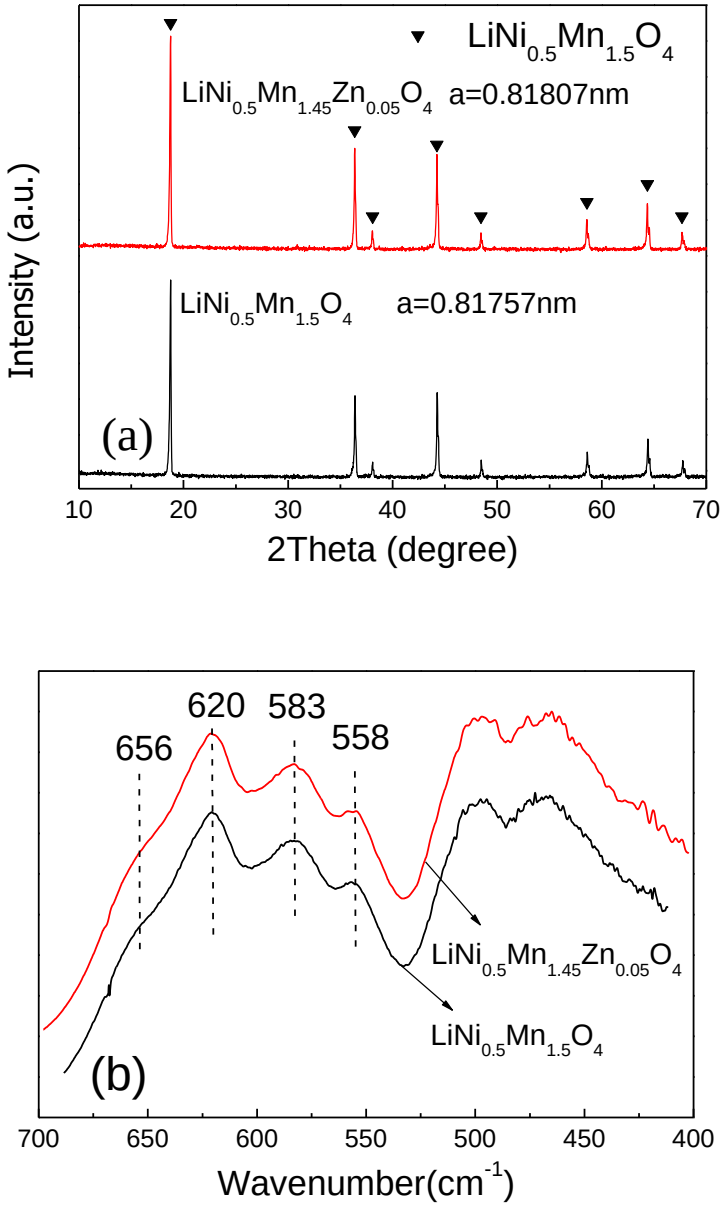

Figure 1. (a) XRD patterns and (b) FT-IR spectra of the products.

Fig. 1 shows the XRD patterns and FT-IR spectra of the products. The XRD results reveal that the products are both well-defined cubic spinels and no obvious trace of impurity phase. The crystal lattice parameter for the $LiNi_{0.5}Mn_{1.45}Zn_{0.05}O_4$ is 0.81807nm which is slightly larger than 0.81757 nm for the $LiNi_{0.5}Mn_{1.5}O_4$. It may be because that the ionic radius of Zn^{2+}(0.074nm) is both larger than that of Mn^{3+}(0.058nm) and Mn^{4+} (0.053nm)[19], suggesting that the Zn^{2+} has been successfully doped into the crystal lattices.

As shown in Fig. 1b, the bands at 558 and 656 cm^{-1} which are the characteristic peaks corresponding to the cation-order $P4_332$ structure basing on a previous reported by L. Wang et al[20]. Meanwhile, the intensity of Ni-O at 583cm^{-1} is lower than that of Mn-O at 620cm^{-1}, indicating that the products also have a degree of cation disorder[21]. So we can assert that the products have a combination structure of ordered $P4_332$ space group and disordered Fd-3m space group, as also observed by Patoux. S et al.[22]. According to the literatures[23, 24], the product with some certain degree of disordered space groups of Fd-3m have better electrochemical performance than with the pure ordered one.

3.2 Micro morphology

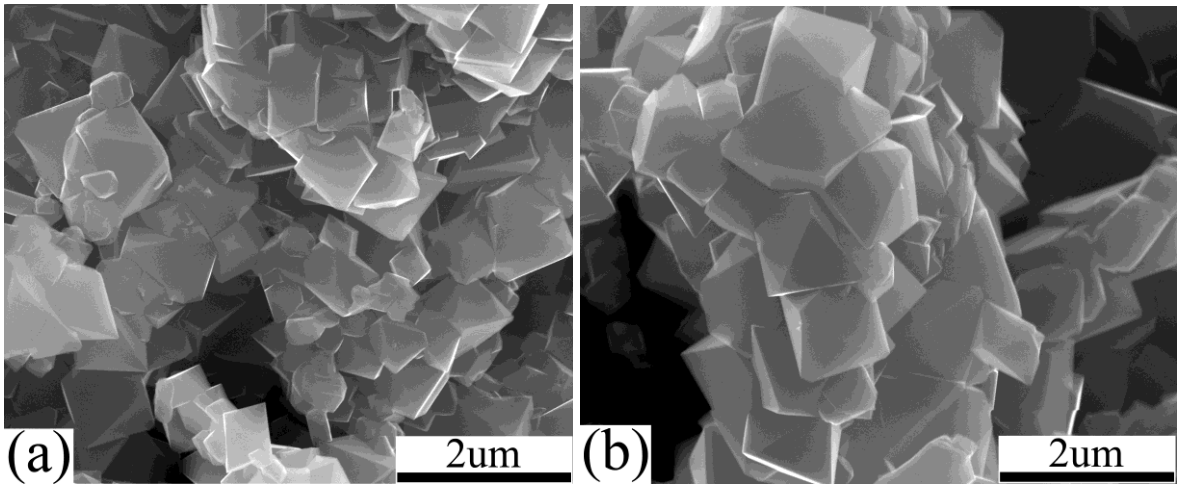

Figure 2. SEM images of (a) $LiNi_{0.5}Mn_{1.5}O_4$ and (b) $LiNi_{0.5}Mn_{1.45}Zn_{0.05}O_4$.

SEM images of the products are displayed in Fig. 2. It can be observed that both samples exhibit perfect octahedral spinel structure. The particles of $LiNi_{0.5}Mn_{1.45}Zn_{0.05}O_4$ are more homogeneous compared with those of $LiNi_{0.5}Mn_{1.5}O_4$ in which some small grains are not fully developed, suggesting that the $LiNi_{0.5}Mn_{1.45}Zn_{0.05}O_4$ is more well-crystallized.

3.3 Electrochemical performance

The initial charge-discharge curves of $LiNi_{0.5}Mn_{1.5}O_4$ and $LiNi_{0.5}Mn_{1.45}Zn_{0.05}O_4$ are shown in Fig. 3. The charge-discharge curves both exhibit two main voltage plateaus in the 4.7V(main) and

4.0V(minor) regions. The appearance of the small plateau at 4V is due to the presence of some Mn^{3+} in the spinel[25].

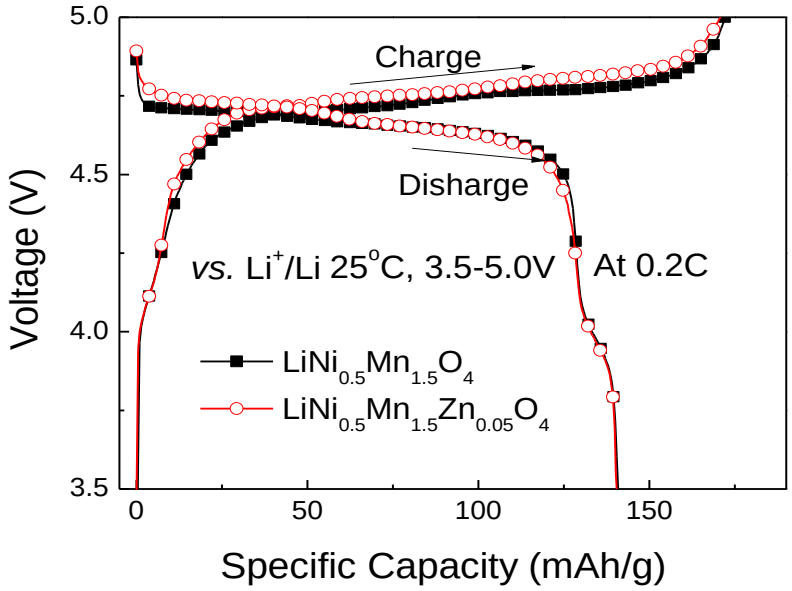

Figure 3. (a) Initial charge-discharge curves of $LiNi_{0.5}Mn_{1.5}O_4$ and $LiNi_{0.5}Mn_{1.45}Zn_{0.05}O_4$

Meanwhile, the 4.0V plateau is very small indicating that the samples don't have single ordered space group but a combination structure of ordered $P4_332$ space group and disordered Fd-3m space group[22], which is in good agreement with above FT-IR results. The initial discharge capacities of the $LiNi_{0.5}Mn_{1.5}O_4$ and $LiNi_{0.5}Mn_{1.45}Zn_{0.05}O_4$ are 140.8 and 140.4mAh/g, respectively. Noticeably, the $LiNi_{0.5}Mn_{1.45}Zn_{0.05}O_4$ doesn't show an obvious capacity degradation as the $LiZn_xNi_{0.5-x}Mn_{1.5}O_4$ reported by Yang et al.[17].

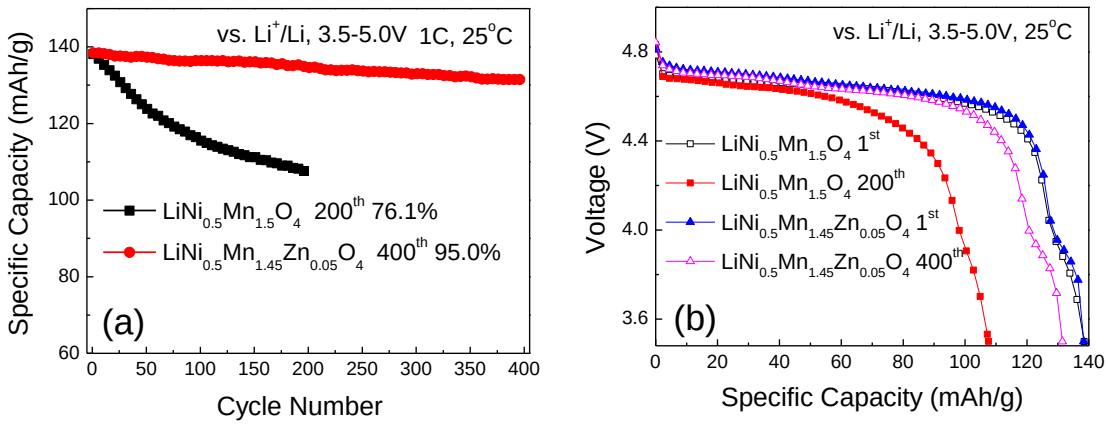

Figure 4. (a) Cycling performance and (b) the discharge curves of the first and the last cycles at 1C rate of $LiNi_{0.5}Mn_{1.5}O_4$ and $LiNi_{0.5}Mn_{1.45}Zn_{0.05}O_4$ at room temperature

In Fig. 4, the cyclic performance and the discharge curves of the first and the last cycles at 1C rate of $LiNi_{0.5}Mn_{1.5}O_4$ and $LiNi_{0.5}Mn_{1.45}Zn_{0.05}O_4$ are shown. It is clearly observed in Fig. 4a that the

cyclic performance of $LiNi_{0.5}Mn_{1.45}Zn_{0.05}O_4$ is superior to that of $LiNi_{0.5}Mn_{1.5}O_4$. The capacity retention of $LiNi_{0.5}Mn_{1.45}Zn_{0.05}O_4$ is 95% after 400 cycles at 1C. In contrast, the capacity retention of $LiNi_{0.5}Mn_{1.5}O_4$ is only 76.1% after merely 200 cycles at the same rate. The results suggest that cyclic performance of $LiNi_{0.5}Mn_{1.5}O_4$ at room temperature can be markedly improved by Zn-doping on Mn site. It is obviously shown in Fig. 4b that there is a very slight drop for the discharge voltage plaform of $LiNi_{0.5}Mn_{1.45}Zn_{0.05}O_4$ after 400 cycles. However, there is a remarkable drop for $LiNi_{0.5}Mn_{1.5}O_4$ after only 200 cycles. Once again shows that the $LiNi_{0.5}Mn_{1.45}Zn_{0.05}O_4$ has an excellent cycling stability. Compared with the Zn doped $LiNi_{0.5}Mn_{1.5}O_4$ on Ni site reported by Yang et al. [17], the cycle stability of the as-prepared products in this paper are much superior. The $LiZn_{0.08}Ni_{0.42}Mn_{1.5}O_4$ prepared by Yang et al. exhibits capacity retention of 95% after only 100 cycles at 0.5C. This result implies that Zn substitution on Mn site is beneficial to the reversible intercalation and deintercalation of Li^+. Compared with $LiNi_{0.5}Mn_{1.5}O_4$ prepared by microwave assist method[26] and improved solid-state method[27], the cycle stability of the $LiNi_{0.5}Mn_{1.45}Zn_{0.05}O_4$ is also superior. The comparison of cycle performance at room temperature is summarized in Table 1.

Table 1. Comparison of cycle performance at room temperature

Literatures	Samples	The capacity retention/%	Testing conditions
Our research	$LiNi_{0.5}Mn_{1.45}Zn_{0.05}O_4$	95	1C, 400th cycle
Reference[26]	$LiNi_{0.5}Mn_{1.5}O_4$	95	1C, 200th cycle
Reference[27]	$LiNi_{0.5}Mn_{1.5}O_4$	81.33	0.2C, 100th cycle

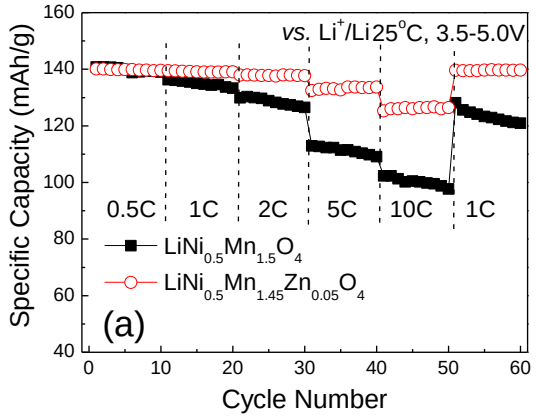

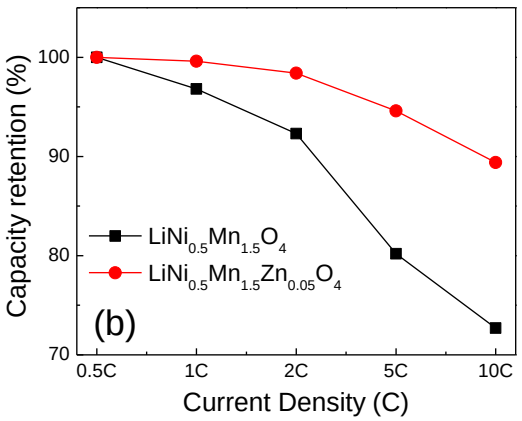

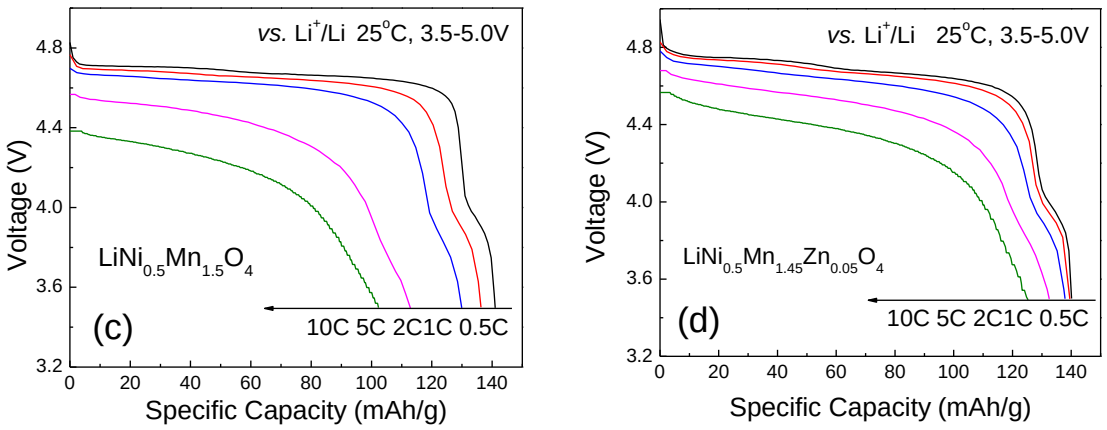

Figure 5. (a) Rate capabilities (b) capacity retentions (c) and (d) discharge curves at different rate of $LiNi_{0.5}Mn_{1.5}O_4$ and $LiNi_{0.5}Mn_{1.45}Zn_{0.05}O_4$ at room temperature.

The rate capability is one of the most important properties for the positive electrode during the practical commercial application for the electric vehicles(EVs) or hybrid electric vehicles(HEVs). To compare the rate capabilities of $LiNi_{0.5}Mn_{1.5}O_4$ and $LiNi_{0.5}Mn_{1.45}Zn_{0.05}O_4$ samples, all coin cells were galvanostatically charged at room temperature under 0.5C and discharged at different C-rates from 0.5C to 10C and then back to 1C (as shown in Fig. 5). The $LiNi_{0.5}Mn_{1.45}Zn_{0.05}O_4$ has much more excellent rate capability than $LiNi_{0.5}Mn_{1.5}O_4$ (shown in Fig. 5a). The capacity of $LiNi_{0.5}Mn_{1.45}Zn_{0.05}O_4$ is 125.3mAh/g at a high rate of 10C. However, the capacity of $LiNi_{0.5}Mn_{1.5}O_4$ exhibits a notable degradation at 2C, and at the rate of 10C, the obtained capacity is only 102.3mAh/g. The capacity retentions at different C rates of the products is shown Fig. 5b.

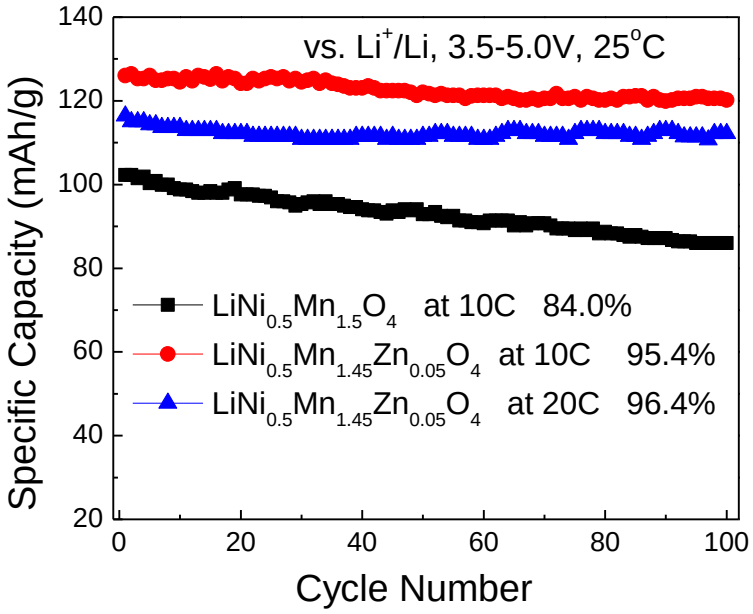

Figure 6. Cycling performance of $LiNi_{0.5}Mn_{1.5}O_4$ and $LiNi_{0.5}Mn_{1.45}Zn_{0.05}O_4$ at 10C rate (and 20C for $LiNi_{0.5}Mn_{1.45}Zn_{0.05}O_4$). Charged at 0.5C, and discharged at 10C or 20C.

The capacity retention rate maintains nearly 89.4% of its capacity compared with 0.5C for the sample $LiNi_{0.5}Mn_{1.45}Zn_{0.05}O_4$ at 10C. On the other hand, the capacity retention of the sample $LiNi_{0.5}Mn_{1.5}O_4$ is only 72.7% at the same rate. The improved rate performance should be attributed to increased electronic conduction by Zn-doping. It can be observed from Fig. 5c and Fig. 5d that the voltage platform of $LiNi_{0.5}Mn_{1.45}Zn_{0.05}O_4$ is obviously higher than that of $LiNi_{0.5}Mn_{1.5}O_4$ at the same high rate(5C~10C).

$LiNi_{0.5}Mn_{1.45}Zn_{0.05}O_4$ displays much better cycle stability at high discharge rates than that of $LiNi_{0.5}Mn_{1.5}O_4$ as demonstrated in Fig. 6. After 100 cycles at 10C, the capacity retention of $LiNi_{0.5}Mn_{1.45}Zn_{0.05}O_4$ is still maintained 95.4% compared with the first cycle at 10C, which is much higher than 84.0% of the $LiNi_{0.5}Mn_{1.5}O_4$ capacity maintained. Meanwhile, the capacity retention of $LiNi_{0.5}Mn_{1.45}Zn_{0.05}O_4$ is nearly 96.4% compared with the first cycle at 20C rate after 100 cycles. Obviously the as-prepared $LiNi_{0.5}Mn_{1.45}Zn_{0.05}O_4$ and $LiNi_{0.5}Mn_{1.5}O_4$ exhibit better rate capacities and cycling performance than many previously reported $LiNi_{0.5}Mn_{1.5}O_4$ spinels[28, 29].

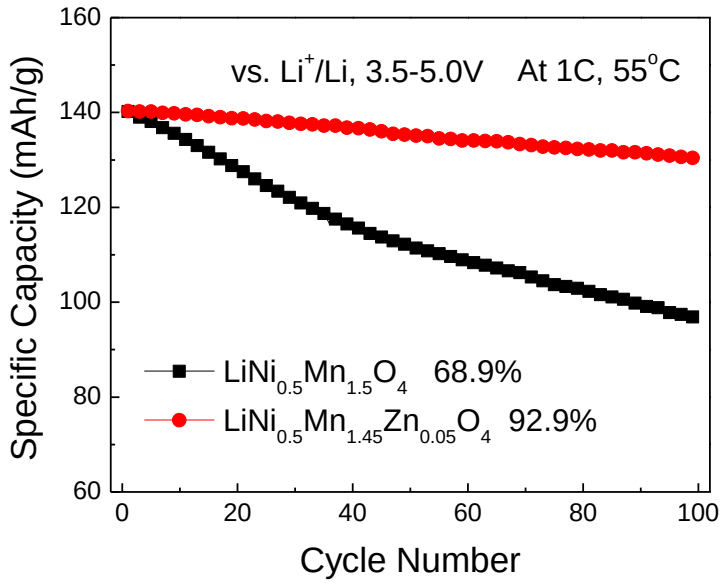

Figure 7. Cycling performance of $LiNi_{0.5}Mn_{1.5}O_4$ and $LiNi_{0.5}Mn_{1.45}Zn_{0.05}O_4$ at 1C and 55 °C.

It is well known that the cyclic performance at elevated temperature(≈55℃) is a very important aspect which effecting the properties of spinel-based positive electrode. The cyclic performances of $LiNi_{0.5}Mn_{1.5}O_4$ and $LiNi_{0.5}Mn_{1.45}Zn_{0.05}O_4$ at 1C rate at 55 °C are shown in Fig. 7. It can be clearly seen that the $LiNi_{0.5}Mn_{1.45}Zn_{0.05}O_4$ sample has excellent cycle stability at elevated temperature. The capacity of $LiNi_{0.5}Mn_{1.5}O_4$ decreases quickly and only retains 68.9% after 100 cycles at 55℃. Nevertheless, the capacity retention of $LiNi_{0.5}Mn_{1.45}Zn_{0.05}O_4$ is high to 92.9% after 100 cycles at the same condition. This demonstrates that Zn doping is helpful to promote the high-temperature cyclic performance for $LiNi_{0.5}Mn_{1.5}O_4$. Although the capacity loss of the two samples at elevated temperature larger than that of at room temperature, they are still better than many other doped $LiNi_{0.5}Mn_{1.5}O_4$ products [30, 31]. The comparison of cycle performance at 55℃ is displayed in Table 2.

Table 2. Comparison of cycle performance at 55℃

Literatures	Samples	The capacity retention/%	Testing conditions
Our research	$LiNi_{0.5}Mn_{1.45}Zn_{0.05}O_4$	92.9	1C, 100th cycle
Reference[30]	$LiNi_{0.5}Mn_{1.5}O_4$	87	1C, 100th cycle
Reference[31]	$LiNi_{0.5}Mn_{1.5}O_4$	90	1C, 50th cycle

.

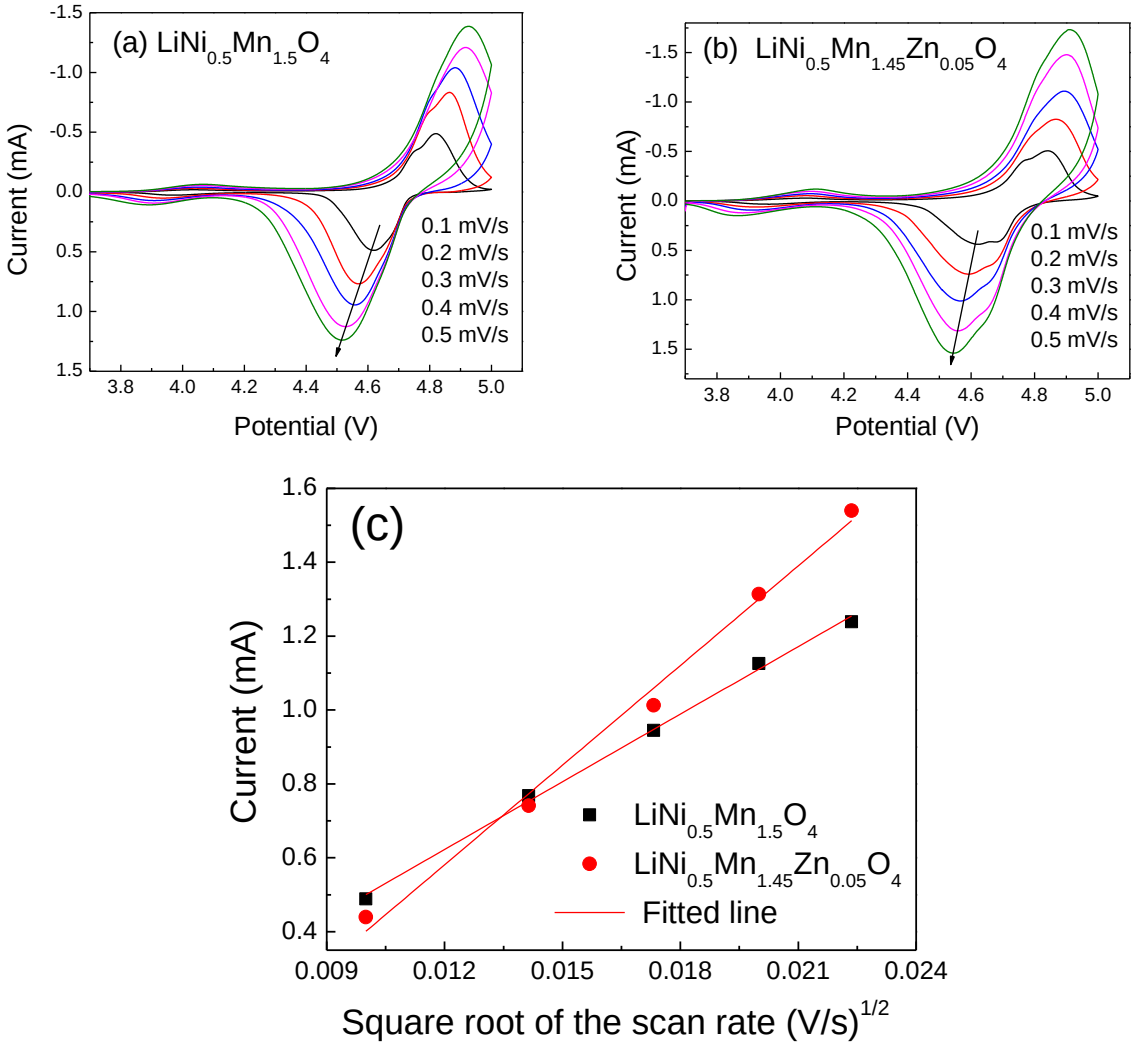

Figure 8. Cyclic voltammograms (CVs) of (a) $LiNi_{0.5}Mn_{1.5}O_4$ and (b) $LiNi_{0.5}Mn_{1.45}Zn_{0.05}O_4$ at different scan rates. (c) The plotting of peak current vs. square root of the scan rate for LNMO-T and LNMO.

The improved high temperature cycle stability for $LiNi_{0.5}Mn_{1.45}Zn_{0.05}O_4$ should be attributed to its high crystallinity and uniform particle size[27]. Meanwhile, some moderate amount of disordered

Fd-3m phase in the material can also suppress the Jahn-Teller distortion and improve structure stability, as reported by Sun et al.[23].

To gain the reason for the excellent electrochemical characteristics of the $LiNi_{0.5}Mn_{1.45}Zn_{0.05}O_4$ sample, we perform a series of voltammetry measurements. Fig. 8a and Fig. 8b show the cyclic voltammograms of $LiNi_{0.5}Mn_{1.5}O_4$ and $LiNi_{0.5}Mn_{1.45}Zn_{0.05}O_4$ recorded at 0.1mV/s-0.5 mV/s scan rates. There are two redox pairs in the CVs at 4.7V and 4.0V regions. The redox peaks mainly located near 4.7V are ascribed to the two-step oxidation/reduction of $Ni^{2+}/Ni^{3+}/Ni^{4+}$. The redox peaks appearing near 4.0V can be attributed to the redox of Mn^{3+}/Mn^{4+} couples. Meanwhile, the redox peaks near 4.0V is very small suggesting that the content of Mn^{3+} is not high. This is well consistent with the discharge curve analysis results above. The cyclic voltammetry (CV) technique can be used to study the diffusion kinetics of Li^+ intercalation/deintercalation and to estimate the diffusion coefficients of $Li^+(D_{Li})$ in solid LNMO electrodes reported by Lantelme et al.[32]. CV peak current shows a square root dependence on the sweep rate. Fig. 8c shows the i_p vs. the square root of the scan rates ($v^{1/2}$) of $LiNi_{0.5}Mn_{1.5}O_4$ and $LiNi_{0.5}Mn_{1.45}Zn_{0.05}O_4$. Both of them display linear increase, which suggests that the intercalation reaction is controlled by solid-state diffusion of lithium-ion[33]. Moreover, the dependence of i_p on $v^{1/2}$ can be applied to approximately determine the diffusion coefficient of Li^+ (D_{Li}) on the basis of the following equation [34]:

$$i_p = 2.69\times10^5 n^{\frac{3}{2}} A C_{Li} D_{Li}^{\frac{1}{2}} \upsilon^{\frac{1}{2}} \qquad (1)$$

Where n is the number of electrons per reaction species (for lithium-ion n=1), A is the total surface area of the electrode (2 cm^2 in this case), and C_{Li} is the bulk concentration of Li^+ in the electrode (given as 0.02378 mol/cm^3) [35]. From the slope of linear fit of i_p vs. v½ in Fig. 8c, the diffusion coefficients (D_{Li}) of $LiNi_{0.5}Mn_{1.5}O_4$ and $LiNi_{0.5}Mn_{1.45}Zn_{0.05}O_4$ have been calculated as $2.27\times10^{-11}cm^2/s$ and $4.93\times10^{-11}cm^2/s$, respectively. The D_{Li} for the products in this paper matches very well with the values reported by other literatures[36, 37]. The D_{Li} value of $LiNi_{0.5}Mn_{1.45}Zn_{0.05}O_4$ is about 2 times larger than that of the $LiNi_{0.5}Mn_{1.5}O_4$. Therefore, the $LiNi_{0.5}Mn_{1.45}Zn_{0.05}O_4$ shows a better rate capability than the $LiNi_{0.5}Mn_{1.5}O_4$.

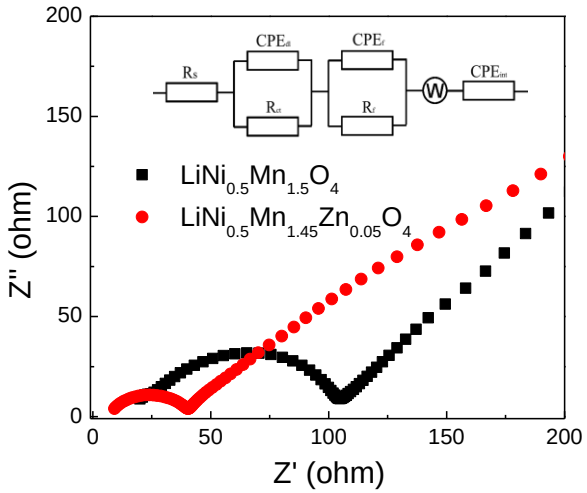

Figure 9. EIS spectra of $LiNi_{0.5}Mn_{1.5}O_4$ and$LiNi_{0.5}Mn_{1.45}Zn_{0.05}O_4$ in the frequency range between 0.1 Hz and 100 kHz.

Fig. 9 shows the electrochemical impedance spectra (EIS) of the batteries with $LiNi_{0.5}Mn_{1.5}O_4$ or $LiNi_{0.5}Mn_{1.45}Zn_{0.05}O_4$ as cathode materials after 3rd cycled and a possible equivalent circuit. The EIS spectrums display the same profile, a depressed semicircle in the high-to-middle frequency region and an inclined line in the low frequency region. The intercept at the Z' axis assigns to the electrolyte resistance (R_s), while the semicircle in high-to-middle frequency region records to the charge transfer resistance (R_{ct}) and the lithium-ion migration resistance (R_f) through the multilayer surface films, and its value can be determined from the diameter of the semicircle[38, 39]. From Fig. 9 it can be seen that the R_{ct} and R_f of $LiNi_{0.5}Mn_{1.45}Zn_{0.05}O_4$ are much smaller than that of $LiNi_{0.5}Mn_{1.5}O_4$ due to the Zn doping, indicating that the former has a much better conductivity than the latter. The lower R_{ct} value of $LiNi_{0.5}Mn_{1.45}Zn_{0.05}O_4$ means a lower electrochemical polarization leading to higher rate capability[7, 40], which is in good agreement with the aforementioned C-rate capacity results.

4. CONCLUSIONS

In this work, a combination structure of ordered and disordered $LiNi_{0.5}Mn_{1.45}Zn_{0.05}O_4$ and $LiNi_{0.5}Mn_{1.5}O_4$ were prepared by modified solution combustion synthesis method at 700℃ for 14h. $LiNi_{0.5}Mn_{1.45}Zn_{0.05}O_4$ shows better cycling stability, better rate capability at fast charge and discharge condition and better elevated temperature cycle performance than those of $LiNi_{0.5}Mn_{1.5}O_4$. The capacity retention of $LiNi_{0.5}Mn_{1.45}Zn_{0.05}O_4$ maintains 95% after 400 cycles at 1C and nearly 96.4% compared with the first cycle at 20C rate after 100 cycles. Moreover, the capacity retention of $LiNi_{0.5}Mn_{1.45}Zn_{0.05}O_4$ is high to 92.9% after 100 cycles at 1C at 55℃. All the results suggested that the as-prepared $LiNi_{0.5}Mn_{1.45}Zn_{0.05}O_4$ could be a promising cathode material for lithium ion batteries.

ACKNOWLEDGEMENT
This work was supported by the National Natural Science Foundation of China(No. 51362012, No. 51662007 and No. U1602273) and the Key Construction Disciplines of Chemistry for Master Degree Program in Yunnan.

References

1. S. Patoux, L. Sannier, H, Lignier, Y. Reynier, C. Bourbon, S. Jouanneau, F.L. Cras and S. Martinet, *Electrochim. Acta* 53 (2008) 4137.
2. H. Li, Z.X. Wang, L.Q. Chen and X.J. Huang, *Adv. Mater*. 21 (2009) 4593.
3. H.M. Wu, J.P. Tu, Y.F. Yuan, Y. Li, X.B. Zhao and G.S. Cao, *Electrochim. Acta* 50 (2005) 4104.
4. Y.K. Sun, K.J. Hong, J. Prakash and K. Amine, *Electrochem. Commun*. 4 (2002) 344.
5. T.F. Yi, J. Mei and Y.R. Zhu, *J. Power Sources* 316 (2016) 85.
6. G.B. Zhong, Y.Y. Wang. Z.C. Zhang and C.H. Chen, *Electrochim. Acta* 56 (2011) 6554.
7. T.F. Yi, Y. Xie, Y.R. Zhu, R.S. Zhu and M.F. Ye, *J. Power Sources* 211 (2012) 59.
8. Z. Zhu, H. Yan, D. Zhang, W. Li and Q. Lu, *J. Power Sources* 224 (2013) 13.
9. G.Y. Liu, X. Kong, H.Y. Sun and B.S. Wang, *Ceram. Int*. 40 (2014) 14391.
10. A. Mauger and C. Julien, *Ionics* 20 (2014) 751.
11. J. Wang, W.Q. Lin, B.H. Wu and J.B. Zhao, *Electrochim. Acta* 145 (2014) 245.

12. G.Y. Liu, H.Y. Sun, X. Kong, Y.N. Li and B.S. Wang, *Int. J. Electrochem. Sci*. 10 (2015) 6651.
13. A. Milewska, L. Kondracki, M. Molenda, M. Bakierska and J. Molenda, *Solid State Ionics* 267 (2014) 27.
14. T.A. Arunkumar and A. Manthiram, *Electrochem. Solid-State Lett*. 8 (2005) A403
15. M. Aklalouch, J.M. Amarilla, I. Saadoune and J.M. Rojo, *J. Power Sources* 196 (2011) 10222.
16. J. Liu and A. Manthiram, *J. Phys. Chem*. C 113 (2009) 15073.
17. Z. Yang, Y. Jiang, J.H. Kim, Y. Wu, G.L. Li and Y.H. Huang, *Electrochim. Acta* 117 (2014) 76.
18. J.H. Kim, N.P.W. Pieczonka, Z. Li, Y. Wu, S. Harris and B.R. Powell, *Electrochim. Acta* 90 (2013) 556.
19. R.L. David, CRC handbook of chemistry and physics, National Institute of Standards and Technology, (2003) New York, the United States.
20. L.P. Wang, H. Li, X.J. Huang and E. Baudrin, *Solid State Ionics* 193 (2011) 32.
21. D.W. Shin, C.A. Bridges, A. Huq, M.P. Paranthaman and A. Manthiram, *Chem. Mater*. 24 (2012) 3720.
22. S. Patoux, L. Daniel, C. Bourbon, H. Lignier, C. Pagano, F.C. Le, S. Jouanneau and S. Martinet, *J. Power Sources* 189 (2009) 344.
23. J.H. Kim, S.T. Myung, C.S. Yoon, S.G. Kang and Y.K. Sun, *Chem. Mater*. 16 (2004) 906.
24. J. Zheng, J. Xiao, X. Yu, L. Kovarik, M. Gu, F. Omenya, X. Chen, X.Q. Yang, J. Liu, G.L. Graff, M.S. Whittingham and J.G. Zhang, *Phys. Chem. Chem. Phys*. 14 (2012) 13515.
25. M. Aklalouch, R.M. Rojas, J.M. Rojo, I.Saadoune and J.M. Amarilla, *Electrochim. Acta* 54 (2009) 7542.
26. X.Y. Feng, C. Shen, H.F. Xiang, H.K. Liu, Y.C. Wu and C.H. Chen, *J. Alloys Compd*. 695 (2017) 227.
27. Y.L. He, J. Zhang, Q. Li, J.W.Yang and C.L. Wang, *J. Alloys Compd.* 715 (2017) 304.
28. D. Liu, J.H. Paquet, J. Trottier, F. Barray, V. Gariepy, P. Hovington, A. Guerfi, A. Mauger, C.M. Julien, J.B. Goodenough and K. Zaghib, J. *Power Sources* 217 (2012) 400.
29. Y.C. Jin, C.Y. Lin and J.G. Duh, *Electhochim. Acta* 69 (2012) 45.
30. J.S. Park, K.C. Roh, J.W. Lee, K. Song, Y. Kim and Y.M. Kang, *J. Power Sources* 230 (2013) 138.
31. M.A. José, M.R. Rosa and M.R. José, *J. Power Sources* 196 (2011) 5951.
32. F. Lantelme, E. Cherrat and *J. Electroanal. Chem. Interfacial Electrochem*. 244 (1988) 61.
33. S.T. Myung, S. Komaba, N. Kumagai, H. Yashiro, H.T. Chung and T.H. Cho, *Electrochim. Acta* 47(2002) 2543.
34. X.H. Rui, N. Ding, J. Liu, C. Li and C.H. Chen, *Electrochim. Acta* 55 (2010) 2384.
35. Y.Y. Xia, H. Takeshige, H. Noguchi and M. Yoshio, *J. Power Sources* 56 (1995) 61.
36. T.Y. Yang, N.Q. Zhang, Y. Lang and K.N. Sun, *Electrochim. Acta* 56 (2011) 4058.
37. A. Ito, D.C. Li, Y.S. Lee, K. Kobayakawa and Y.C. Sato, *J. Power Sources* 185 (2008) 1429.
38. X.L. Li, W. Guo, Y.F. Liu, W.X. He and Z.H. Xiao, *Electrochim. Acta*, 116 (2014) 278.
39. J. Liu and A. Manthiram, *Chem. Mater*. 21 (2009) 1695.
40. Y.Z. Wang, X. Shao, H.Y. Xu, M. Xie, S.X. Deng, H. Wang, J.B. Liu and H. Yan, *J. Power Sources* 226 (2013) 140.